Bioorganic & Medicinal Chemistry 28 (2020) 115527

Contents lists available at ScienceDirect

Bioorganic & Medicinal Chemistry

journal homepage: www.elsevier.com/locate/bmc

Secondary metabolites from *Isodon ternifolius* (D. Don) Kudo and their anticancer activity as DNA topoisomerase IB and Tyrosyl-DNA phosphodiesterase 1 inhibitors

Hong-Li Zhang[a], Yu Zhang[a], Xue-Long Yan[a], Long-Gao Xiao[a], De-Xuan Hu[a], Qian Yu[a,b,*], Lin-Kun An[a,c,*]

[a] School of Pharmaceutical Sciences, Sun Yat-sen University, Guangzhou 510006, China
[b] Clinical Pharmacy (School of Integrative Pharmacy, Institute of Integrative Pharmaceutical Research), Guangdong Pharmaceutical University, Guangzhou 510006, China
[c] Guangdong Provincial Key Laboratory of New Drug Design and Evaluation, Guangzhou 510006, China

ARTICLE INFO

Keywords:
Isodon ternifolius
Secondary metabolite
DNA topoisomerase
Tyrosyl–DNA phosphodiesterase
Cytotoxicity

ABSTRACT

Ce, and **22** acted as TOP1 catalytic inhibitors with equipotent TOP1 inhibition to camptothecin (+ + + +). Compounds **7** and **8** exhibited significant cytotoxicity against MCF-7, A549, and HCT116 cells with GI

$_{50}$ values in the range of 2.2–4.8 μM. This work would provide valuable information that secondary metabolites from *I. ternifolius* could be developed as anticancer agents.

1. Introduction

DNA topoisomerase IB (TOP1) is an essential enzyme that regulates DNA topological structure in many cellular metabolic processes including replication and transcription.[1] TOP1 is a validated molecular target for the discovery of anticancer agent.[2,3] TOP1 inhibitors are classified into two types as TOP1 "poisons" and "catalytic inhibitors" based on their molecular mechanism of action. TOP1 poisons can stabilize the enzyme-DNA covalent complexes (TOP1cc) to prevent further relegation and lead to DNA single-strand breaks.[4,5] Camptothecin (CPT) and their derivatives are the classical TOP1 poisons. To date, four well-known CPT derivatives have been approved for clinical treatment of cancers.[6–8] Unlike TOP1 poisons, catalytic inhibitors act at the upstream stage of the catalytic DNA cleavage reaction of TOP1, and prevent the formation of TOP1cc by blocking the nucleophilic attack of the scissile strand.[9] Several catalytic inhibitors from natural products have been already discovered.[10–12]

Tyrosyl-DNA phosphodiesterase 1 (TDP1) is a DNA repair enzyme that specifically hydrolyzes 3′-phosphotyrosyl bond derived from TOP1cc and repairs TOP1-induced DNA damages.[13,14] resulting in cancer cells resistant to TOP1 inhibitors.[15] Therefore, inhibition of TDP1 could potentiate the anticancer e□cacy of TOP1 inhibitors. Indeed, several previous studies reported that TDP1 inhibitors exhibit synergistic e□ect to TOP1 inhibitors.[16,17] Therefore, TDP1 is a rational target for the development of anticancer agents.[14,18,19]

Because of the unique biological functions of TOP1 and TDP1, the discovery of their inhibitors has attracted attentions. However, there is only two kind of dual inhibitors reported now.[17,20] In our study for anticancer agents from natural products, the ethanol extract of the roots of *Isodon ternifolius* (D. Don) Kudo (Labiatae) showed strong TOP1 inhibition at 50 μg/mL (Fig. S1) and TDP1 inhibitory activity (85% inhibition at 100 μg/mL), which inspired us to study its secondary metabolites.

I. ternifolius is perennial subshrubs to shrubs widely distributed in the southwestern region of China.[21] *I. ternifolius* has been commonly used as folk medicine to treat dysenteric enteritis, icterohepatitis, and inflammatory ailments.[22,23]*I. ternifolius* is also the major ingredient of a Chinese patent medicine "Fufang Sanyexiangchacai Pian", which is

* Corresponding authors at: School of Pharmaceutical Sciences, Sun Yat-sen University, Guangzhou 510006, China.
E-mail addresses: yuxi3@mail.sysu.edu.cn (Q. Yu), lssalk@mail.sysu.edu.cn (L.-K. An).

https://doi.org/10.1016/j.bmc.2020.115527
Received 27 February 2020; Received in revised form 17 April 2020; Accepted 20 April 2020
Available online 22 April 2020

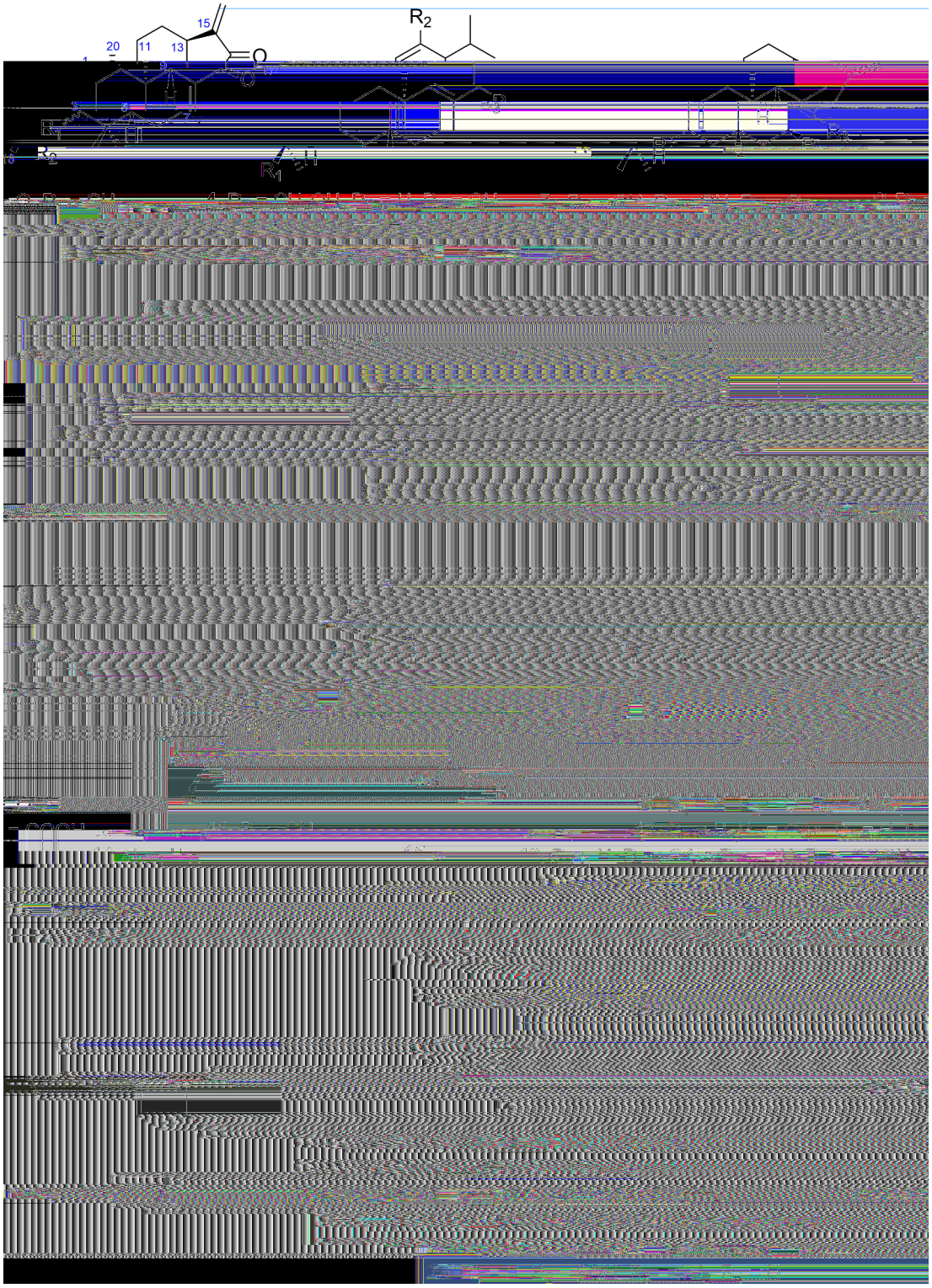

Fig. 1. Chemical structures of **1**–**27** isolated from the roots of *I. ternifolius.*

used to treat acute and chronic hepatitis and hepatitis B. Its secondary metabolite oridonin exhibits significant anticancer activity for human breast cancer,[24] gallbladder cancer,[25] leukemia,[26] and gastric cancer.[27] In addition, previous phytochemical studies on this plant have revealed that *ent*-kaurane diterpenes, ursanes and oleananes triterpenoids are its main secondary metabolites, some of which show anti-inflammatory,[28] antioxidative,[29] and anticancer activities.[30] In this work, we report the isolation and structure elucidation of the compounds isolated from this plant, and their biological evaluations.

2. Results and discussion

2.1. Phytochemical investigation

The air-dried powder of the roots of *I. ternifolius* was extracted with 95% EtOH at room temperature to give a crude extract, which was

Table 1
^{1}H (500 MHz) and ^{13}C (125 MHz) NMR data of **1** in $CDCl_3$.

No.	δ_H (mult., *J* in Hz)	δ_C, type	No.	δ_H (mult., *J* in Hz)	δ_C, type
1	2.12, m 1.10, dd (14.0,4.0)	37.6, CH_2	11	1.74, m 1.74, m	21.9, CH_2
2	2.69, m 2.29, dd (14.7, 3.8)	34.6, CH_2	12	α1.86, m β1.38, m	29.1, CH_2
3		216.1, C	13	2.97, ddd (10.8, 5.8, 5.8)	41.1, CH
4		47.4, C	14	4.75, d (5.5)	81.9, CH
5	1.70, m	50.4, CH	15		141.7, C
6	2.16, m 2.12, m	24.4, CH_2	16	6.15, s 5.58, s	120.8, CH_2
7	6.07, m	133.1, CH	17		170.4, C
8		131.6, C	18	1.08, s	25.5, CH_3
9	2.01, dd (8.7, 5.9)	47.4, CH	19	1.12, s	22.6, CH_3
10		35.2, C	20	1.01, s	14.2, CH_3

suspended in H_2O and partitioned with EtOAc. Various column chromatographic separations of the EtOAc fraction a□orded twenty seven compounds (Fig. 1), including two new compounds (**1** and **13**) and twenty five known compounds (**2**–**12** and **14**–**27**).

Isodopene A (**1**) was obtained as white powder. Its molecular formula $C_{20}H_{26}O_3$ was determined by the positive HRESIMS ion at *m/z* 337.1771 [M + Na]$^+$ (calcd for $C_{20}H_{26}O_3Na^+$, 337.1774). The IR spectrum revealed the presence of the carbonyl groups (1762 and 1707 cm^{-1}). The ^1H NMR data of **1** displayed signals for three methyl groups [δ_H 1.01 (3H, s), 1.08 (3H, s) and 1.12 (3H, s)], a terminal double bond [δ_H 5.58 (1H, s) and 6.15 (1H, s)], an olefinic proton [δ_H 6.07 (1H, m)], an oxymethine proton [δ_H 4.75 (1H, d, *J* = 5.5 Hz)], and a series of aliphatic multiplets (Table 1). The ^{13}C NMR spectrum (Table 1), associated with DEPT NMR spectrum, displayed 20 distinct carbon resonances attributed to a ketone carbonyl (δ_C 216.1), an ester carbonyl group (δ_C 170.4), a terminal double bond (δ_C 120.8 and 141.7), a trisubstituted double bond (δ_C 131.6 and 133.1), three methyl groups (δ_C 14.2, 22.6, and 25.5), four methines (one oxygenated at δ_C 81.9), five methylenes, and two quaternary carbons (δ_C 35.2 and 47.4). The above mentioned information was similar to that of a co-isolated *ent*-abietane diterpenoid **3** (isoforrethin C),[37] except for the major differences being due to the presence of an additional ketocarbonyl group (δ_C 216.1, C-3) and the absence of the oxymethine carbon in **1**, suggesting that **1** was an oxidized derivative of **3**. The location of the ketocarbonyl group was assigned at C-3 according to the HMBC correlations from H_3-18 and H_3-19 to ketocarbonyl (Fig. 2). The detailed 2D NMR data analysis confirmed the planar structure of **1**, which could be further confirmed through the oxidization of **3** with PCC in dichloromethane.

The relative configuration of **1** was established by NOESY experiments and $^1H-^1H$ coupling constants. The strong NOE corrections of H-5/Me-18 and Me-20/Me-19, along with the absence of NOE correlation between H-5 and Me-20 suggested the *trans*-relationship of H-5 and Me-20, and they occupied the axial bonds of the chair conformational cyclohexanone ring A. Thus, H-5 was arbitrarily designated as β-orientation, while Me-20 was accordingly assigned as α-orientation. Then, the NOE correlations of H-9/H-5 and H-12β assigned that H-9 was β-oriented. Subsequently, the NOE correlations H-13/H-12α and H-13/H-14 assigned H-13 and H-14 to be α-orientation. This assignment was also supported by the coupling constants of H-13 (ddd, *J* = 10.8, 5.8, 5.8 Hz) and H-14 (d, *J* = 5.5 Hz) on the chair conformational C ring. Moreover, the absolute configuration of **1** was established by comparing its experimental ECD spectra with those calculated by the time-dependent density functional theory (TDDFT). As shown in Fig. 3, the experimental ECD curve of **1** showed a negative Cotton e□ect at 212 nm, indicating that **1** had a (5*S*,9*S*,10*S*,13*S*,14*R*)-configuration. Thus, compound **1** was established as depicted, and was given a trivial name isodopene A.

Isodopene B (**13**) was obtained as white powder. The HRESIMS ion at *m/z* 525.3560 [M + Na]$^+$ (calcd for $C_{31}H_{50}O_5Na$, 525.3550) suggested a molecular formula $C_{31}H_{50}O_5$ for **13**. The IR spectrum showed absorption of hydroxyl group (3337 cm^{-1}) and carbonyl group (1736 cm^{-1}). The ^1H NMR data of **13** showed signals of seven methyl groups [δ_H 0.78 (3H, s), δ_H 0.80 (3H, s), 0.94 (3H, d, *J* = 6.6 Hz), 0.98 (3H, s), 1.12 (3H, s), 1.19 (3H, s), 1.23 (3H, s)], a methoxyl group [δ_H 3.33 (3H, s), two oxygenated methylene protons [δ_H 3.03 (1H, d, *J* = 12.8 Hz) and 3.78 (1H, d, *J* = 12.9 Hz)], an hemiacetal proton [δ_H 4.57 (1H, dd, *J* = 9.4, 5.0 Hz)], an olefinic proton [δ_H 5.36 (1H, dd, *J* = 3.9, 3.9 Hz)] (Table 2). The ^{13}C NMR spectrum (Table 2), associated with DEPT NMR spectrum, classified thirty one carbon resonances for a carboxyl group (δ_C 184.0), a trisubstituted double bond (δ_C 129.9 and 137.9), a hemiketal carbon (δ_C 101.1), four methines, seven methyls, nine methylenes (one oxygenated at δ_C 70.6), an oxygenated tertiary carbon (δ_C 73.2), and five sp^3 quaternary carbons. The abovementioned information showed high similarity with that of a co-isolated 2,3-seco-triterpene **14** (maquatic acid),[38] except for the presence of an additional methoxyl group in **13**, indicating that **13** was a methylated derivative of **14**. HMBC correlation from H-2 to the methoxyl carbon (δ_C 54.6) located the methoxyl group at C-2. Further detailed analysis of the 2D NMR data confirmed the planar structure of **13**.

The stereochemistry of **13** was determined by analysis of its NOESY correlations. The NOESY correlations of H-9/H-5 and Me-26/Me-25 suggested that H-5, H-9, Me-26, and Me-25 occupied the axial bonds of the chair conformational B ring (Fig. 2). Thus, H-5 and H-9 were arbitrarily designated as α-orientations, while Me-26 and Me-25 were accordingly assigned as β-orientation. Subsequently, the NOE correlations Me-25/H-2 suggested that H-2 was β-orientation. The NOE correlations H-9/Me-27, Me-27/H-16α, and H-16α/H-22α indicated that Me-27 was α-orientation. Thus, on the chair conformational E ring, the NOE correlations of H-18/H-22β, Me-29, and H-20 assigned H-18, Me-29, and H-20 to be β-orientation.

The absolute configuration of **13** was established by comparing its experimental ECD spectra with those calculated by the time-dependent density functional theory (TDDFT). As shown in Fig. 3, the experimental ECD curve of **13** showed one positive (187 nm) and one negative (233 nm) Cotton e□ects, respectively, indicating that **13** had a (2*S*,5*R*,8*R*,9*R*,10*R*,14*S*,17*S*,18*S*,19*R*,20*R*)-configuration. Thus, compound **13** was established as depicted, and was given a trivial name isodopene B.

The 25 known compounds were identified as isoforrethin D (**2**),[37] isoforrethin C (**3**),[37] macrophynin E (**4**),[38] 19-hydroxyferruginol (**5**),[39] (−)-lambertic acid (**6**),[38] 3α,7β-dihydroxy-*ent*-kaur-16-en-15-one (**7**),[40] *ent*-3α-hydroxykaurene-15-one (**8**),[41] inumakoic acid (**9**),[42] trogopteroid F (**10**),[43] isoliquiritigenin (**11**),[44] echinatin (**12**),[45] maquatic acid (**14**),[46] ursolic acid lactone (**15**),[47] 3-oxo-urs-12-en-28-oic acid (**16**),[48] 2,4 ursolic acid acetate (**17**),[49] pomolic acid 3β-acetate (**18**),[50] 3β,28-dihydroxyursulane (**19**),[51] euscaphic (**20**),[52] corosolic acid (**21**),[53] eucalyptolic acid (**22**),[54] epimaslinic acid (**23**),[55] 2α,3β,24-trihydroxyolean-12-en-28-oic acid (**24**),[56] 2β-hydroxy-23–(2-isopropanoloxy)-oleanolic acid (**25**),[41] 2α,3α,23-trihydroxy-olean-12-en-28-oic acid (**26**),[57] and oleanolic acid (**27**)[58] by comparison of their NMR data with those in the literature.

2.2. TDP1 inhibition

The isolates were firstly screened for their TDP1 inhibition through a fluorescence assay at 100 μM concentration. Twenty-one compounds **1**–**12**, **14**, **17**–**23**, and **25** showed TDP1 inhibition with the percentage inhibition ranging from 20% to 99%. These twenty-one active compounds were further tested for IC_{50} values, defined as the compound concentration that results in 50% enzyme activity inhibition. As shown in Table 3, most compounds showed low TDP1 inhibitory activity with IC_{50} values more than 100 μM except two chalcone derivatives

Fig. 2. Key 2D NMR correlations of **1** and **13**.

isoliquiritigenin (**11**) and echinatin (**12**) showing moderate inhibition with IC_{50} values of 55 μM and 45 μM, respectively.

2.3. TOP1 inhibition

TOP1 inhibitory activity of the isolates was assessed by TOP1-mediated relaxation assay with CPT as a positive control, and semi-quantitatively expressed relative to CPT at 100 μM as follows: + + + +, more than 90% of the activity; + + +, between 60% and 89% of the activity; + +, between 30% and 59% of the activity; +, less than 29% of the activity; 0, no activity. As shown in Table 3, five compounds **8**, **16**, **17**, **20**, and **22** exhibited equipotent inhibitory activity to CPT with TOP1 inhibition of + + + + (Fig. 4A). Compounds **8**, **16**, and **22** showed well dose-dependent inhibition of TOP1 at the concentrations of 0.4, 2, 10, 50, and 250 μM. Four compounds **1**, **7**, **24**, and **25** showed high TOP1 inhibition of + + +. Eleven compounds, including the new compound **13** and the most potent TDP1 inhibitors **11** and **12** showed moderate TOP1 inhibition (+ +).

To study the inhibitory mechanism of the active compounds, **8**, **16**, and **22** were selected for further studies. TOP1 poison CPT could trap and stabilize TOP1cc and was used as the positive control. TOP1-mediated DNA cleavage assay indicated that the nicked DNA content increased in the lanes with the presence of CPT (Fig. 4B). With the presence of **8**, **16**, and **22**, the nicked DNA content decreased, implying that these compounds could inhibit the formation of TOP1cc. TOP1-mediated EMSA assay (Fig. 4C) indicated that the tested compounds did not hamper the binding of TOP1 to DNA. The TOP1-mediated assays indicated that the compounds **8**, **16**, and **22** act as TOP1 catalytic inhibitors, which prevent the formation of TOP1-DNA covalent cleavage complex by blocking the nucleophilic attack of TOP1 to the scissile strand.

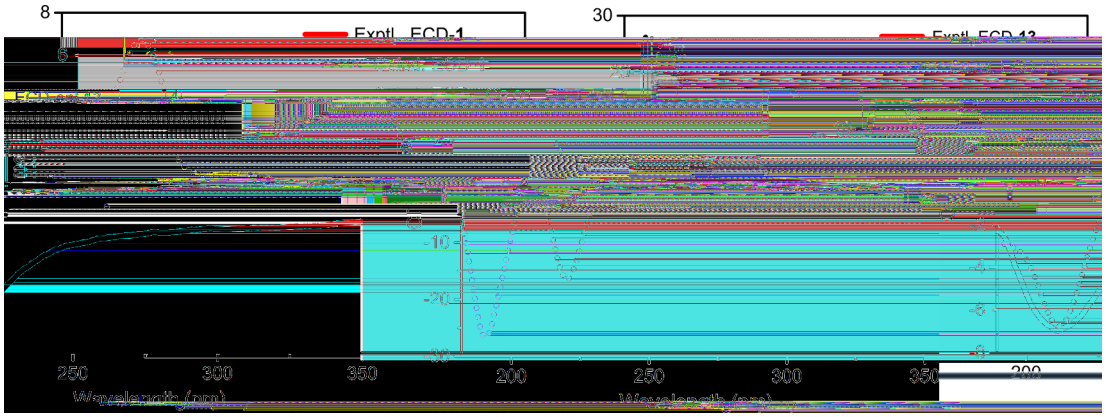

Fig. 3. Calculated and experimental ECD spectra of **1** and **13** in MeCN.

Table 2
^{1}H (500 MHz) and ^{13}C (125 MHz) NMR data of **13** in $CDCl_3$.

No.	δ_H (mult., *J* in Hz)	δ_C, type	No.	δ_H (mult., *J* in Hz)	δ_C, type
1	2.05, m	43.9, CH_2	15	1.70, m	28.3, CH_2
	1.39, m			1.04, m	
2	4.57, dd (9.4, 5.0)	101.1, CH	16	β2.51, m	25.6, CH_2
				α1.60, m	
			17		48.0, C
3	3.78, d (12.9)	70.6, CH_2	18	2.54, s	53.1, CH
	3.03, d (12.8)		19		73.2, C
4		39.2, C	20	1.41, m	41.2, CH
5	0.83, m	60.1, CH	21	1.68, m	26.1, CH_2
				1.31, m	
6	1.47, m	20.9, CH_2	22	α1.80, m	37.5, CH_2
	1.36, m			β1.67, m	
7	1.46, m	33.0, CH_2	23	0.80, s	28.0, CH_3
	1.31, m				
8		40.7, C	24	0.98, s	21.1, CH_3
9	1.59, m	44.2, CH	25	1.12, s	14.2, CH_3
			26	0.78, s	17.6, CH_3
10		40.8, C	27	1.23, s	24.4, CH_3
11	2.12, m	24.8, CH_2	28		184.0, C
	1.99, m				
12	5.36, dd (3.9, 3.9)	129.9, CH	29	1.19, s	27.5, CH_3
13		137.9, C	30	0.94, d (6.6)	16.3, CH_3
14		41.8, C	$-OCH_3$	3.33, s	54.6, CH_3

Table 3
The TDP1 and TOP1 inhibitory activities, and the cytotoxicity of the isolated compounds.

No.	Inhibition		Cytotoxicity (GI_{50}, μM)[c]		
	TDP1[a]	TOP1[b]	MCF-7	A549	HCT116
1	> 100	+ + +	15 ± 5.6	51 ± 1.7	31 ± 0.4
2	No[d]	+ +	40 ± 1.4	51 ± 2.1	42 ± 3.2
3	> 100	+ +	53 ± 5.1	35 ± 1.1	35 ± 3.2
4	> 100	0	> 100	> 100	> 100
5	> 100	+ +	92 ± 2.4	91 ± 3.0	51 ± 1.7
6	> 100	+ +	60 ± 5.9	36 ± 2.2	68 ± 3.3
7	> 100	+ + +	3.5 ± 0.4	4.8 ± 0.5	2.7 ± 0.3
8	> 100	+ + + +	2.2 ± 1.1	3.0 ± 0.4	2.8 ± 0.4
9	> 100	+ +	60 ± 2.2	41 ± 14	31 ± 7.1
10	> 100	+ +	49 ± 2.3	24 ± 0.9	43 ± 3.1
11	55 ± 0.4	+ +	> 100	87 ± 2.8	39 ± 4.3
12	45 ± 0.5	+ +	43 ± 1.2	36 ± 1.2	64 ± 4.4
13	> 100	+ +	31 ± 1.5	63 ± 2.5	37 ± 8.3
14	> 100	+	> 100	> 100	23 ± 5.1
15	No	0	> 100	> 100	> 100
16	No	+ + + +	12 ± 0.9	57 ± 4.1	5.3 ± 0.8
17	> 100	+ + + +	6.5 ± 2.0	48 ± 1.6	21 ± 3.7
18	> 100	0	> 100	> 100	> 100
19	> 100	+ +	93 ± 6.1	45 ± 2.4	37 ± 1.5
20	> 100	+ + + +	41 ± 5.0	43 ± 8.4	22 ± 3.6
21	> 100	+	62 ± 8.1	> 100	> 100
22	> 100	+ + + +	67 ± 2.1	59 ± 3.7	22 ± 2.8
23	> 100	+ +	> 100	> 100	51 ± 1.3
24	No	+ + +	14 ± 0.02	22 ± 1.3	29 ± 2.0
25	> 100	+ + +	11 ± 1.1	37 ± 2.8	55 ± 3.0
26	No	0	> 100	> 100	> 100
27	No	0	> 100	> 100	> 100

[a] TDP1 inhibition was determined by using a fluorescence assay and expressed as IC_{50} (μM) values. Every experiment was repeated at least three times independently.

[b] Top1 inhibitory activity was semiquantitatively expressed relative to CPT at 100 μM as follows: + + + +, > 90% of the activity; + + +, between 60% and 89% of the activity; + +, between 30% and 59% of the activity; +, less than 29% of the activity; 0, no activity.

[c] GI_{50} values were defined as the concentrations of compounds resulting in 50% cell growth inhibition. Every experiment was repeated at least three times independently.

[d] No TDP1 inhibitory activity at 100 μM concentration.

2.4. Cytotoxicity

The cytotoxicity of the isolates was evaluated through MTT assay against three human cancer cell lines, including breast cancer (MCF-7), non-small cell lung cancer (A549), and colon cancer (HCT116) cell lines. The GI_{50} values, defined as the concentrations resulting in 50% cell growth inhibition, are summarized in Table 3. The potent TOP1 inhibitors, *ent*-kaurane diterpenoids **7** (+ + +) and **8** (+ + + +) displayed significant cytotoxicity against three human cancer cells with GI_{50} values ranging from 2.2 to 4.8 μM. Compound **16** showed high cytotoxicity against HCT116 (GI_{50} = 5.3 μM) with TOP1 inhibition of + + + +. Compound **17** showed high cytotoxicity against MCF-7 cells (GI_{50} = 6.5 μM) with TOP1 inhibition of + + + +. Although compounds **20** and **22** had potent TOP1 inhibition (+ + + +), they showed moderate cytotoxicity against these three cancer cells.

2.5. Synergistic e ect

Because the chalcone derivatives **11** and **12** showed moderate TDP1 inhibition, their synergistic activity with the TOP1 poison topotecan (TPT) was evaluated in MCF-7 cells by using MTT assay. After being incubated for 72 h at 37 °C, the cytotoxicity of TPT against MCF-7 Cells significantly increased in the presence of both **11** and **12** (Fig. 5, left). The combination analyses of the does-response data were presented in form of Combination Index (CI) vs. Fraction A□eted (Fa) plots (Fig. 5, right), demonstrating that **11** showed synergistic e□ect (CI values < 1) and **12** showed strong synergistic e□ect with TPT (CI values < 0.3) in MCF-7 cells.

2.6. DNA damage

To assess the DNA damage e□ect, γH2AX foci formation induced by **8** and **16** was conducted by immunofluorescence microscopy in breast cancer MCF-7 cells. After being incubated with **8** and **16** for 12 h, MCF-7 cells were stained with γH2AX antibodies. As shown in Fig. 6, positive control CPT could e□ectively induce γH2AX foci formation at 0.5 μM concentration. On the contrary, there were only weak DNA damage observed after being incubated with **8** or **16** up to 9 μM concentration, implying that both **8** and **16** could not induce TOP1-mediated DNA break which is consistent with their molecular action for TOP1.

3. Conclusion

In summary, twenty-seven compounds, including a new *ent*-abietane diterpenoid (**1**) and a new 2,3-*seco*-triterpene (**13**) were isolated from the EtOH extract of the roots of *I. ternifolius*. The two new compounds **1** and **13** showed strong and moderate TOP1 inhibition of + + + and + +, respectively. To the best of our knowledge that two chalcone derivatives **11** and **12** were firstly found as dual TDP1 and TOP1 natural inhibitors, and showed synergistic e□ect with TPT in MCF-7 cells. Five compounds **8**, **16**, **17**, **20**, and **22** showed strong TOP1 inhibitory activity of + + + +. Further studies indicated that compounds **8**, **16**, and **22** could prevent the formation of covalent cleavage complex acting as TOP1 catalytic inhibitors, and antagonize TOP1-mediated DNA break in MCF-7 cells. Compound **8** exhibited the highest cytotoxicity against MCF-7 and A549 cells with GI_{50} value of 2.2 and 3.0 μM, respectively. Compound **7** showed the highest cytotoxicity against HCT116 cells with GI_{50} value of 2.7 μM. These results imply that *I. ternifolius* have multiple health functions, and will attract more attention for food scientists because it is consumed as cattle feed and has nutritional and pharmaceutical values.

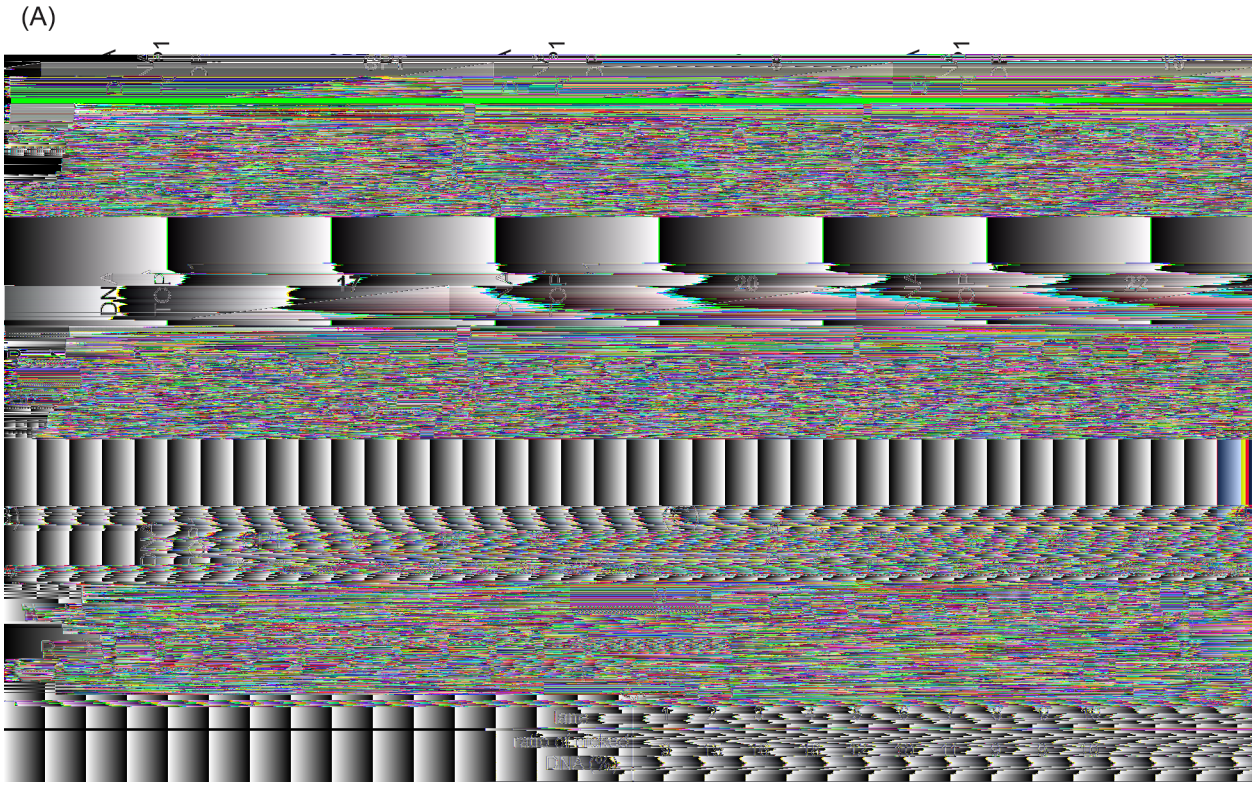

Fig. 4. (A) TOP1-mediated relaxation assays. Lane 1, pBR322 DNA alone; lane 2, pBR322 DNA and TOP1; lanes 3–7, pBR322 DNA, TOP1 and CPT at 0.2, 1, 5, 25, 125 μM, or the tested compounds at 0.4, 2, 10, 50, 250 μM concentrations, respectively. (B) TOP1-mediated DNA cleavage assays. Lane 1 pBR322 DNA alone; lane 2, pBR322 DNA and TOP1; lanes 3–10, pBR322 DNA, TOP1 and the drugs at 25 and 50 μM concentrations, respectively. (C) DNA mobility shift analysis. Lane 1, pBR322 DNA alone; lane 2, pBR322 DNA and TOP1; lanes 3–10, pBR322 DNA, TOP1 and the drugs at 25 and 50 μM concentrations, respectively. R, relaxed DNA; Sc, supercoiled DNA; N, nicked DNA; C, TOP1-bound DNA.

4. Materials and methods

4.1. General experimental procedures

Optical rotations were measured on a Perkin-Elmer 341 polarimeter (PerkinElmer, Inc. Shelton, USA). Melting points were measured on an X-5 melting instrument without being corrected. UV spectra were recorded on a Shimadzu UV-2450 spectrophotometer. IR spectra were determined on a Bruker Tensor 37 infrared spectrophotometer with KBr pellets. CD spectra were obtained on an Applied Photophysics Chirascan spectrometer. HRESIMS were measured on a Shimadzu LCMS-IT-TOF spectrometer. Nuclear magnetic resonance spectra were measured on a Bruker AM-500 spectrometer using tetramethylsilane as an internal reference. A SEP LC-52 equipped with UV-200 and a Dr. Maisch C_{18} column (250 × 10 mm, S-5 μm) was used for semi-preparative HPLC separation. RP-C_{18} silica gel (YMC, 50 μm), MCI gel (CHP20P, 75–150 μm, Mitsubishi Chemical Corporation, Tokyo, Japan), silica gel (100–200 and 200–300 Mesh Marine Chemical Ltd, Qingdao, People's Republic of China), and sephadex LH-20 (GE Healthcare Bio-Sciences AB, Sweden) were used for column chromatography (CC). TLC was carried out on silica gel GF_{254} plates (Qingdao Marine Chemical, Inc. China). All solvents were analytical grade from the local suppliers without further purification. TDP1 protein was expressed and purified from *Escherichia coil* BL21 (DE3) cells in our lab. Plasmid pBR322 DNA and calf thymus DNA TOP1 were purchased from Takara Biotechnology (Dalian, People's Republic of China). A549, HCT116 and MCF-7 cell lines were purchased from China Center for Type Culture Collection.

4.2. Plant material

The roots of *I. ternifolius* were collected in June from Yulin county, Guangxi province, People's Republic of China, and identified by Dr. Gui-Hua Tang, Sun Yat-sen University. A voucher specimen (No. 2018121101) was deposited at the School of Pharmaceutical Sciences, Sun Yat-sen University.

4.3. Extraction and isolation

The air-dried powder of the roots of *I. ternifoliu* (20 kg) was extracted with 95% EtOH (20 L × 3) at room temperature to give a crude extract (3 kg). The crude extract was suspended in H_2O (2.5 L) and partitioned with EtOAc (5 L × 3). The EtOAc fraction (506 g) was subjected to silica gel CC eluted with a petroleum ether/EtOAc gradient (100:1 to 0:1, v/v) to obtain ten fractions (Fr.A − Fr.J). Fr.I was separated by RP-18 silica gel CC, eluted with MeOH/H_2O gradient (30% to 100%, v/v) to give four subfractions (Fr.Ia − Fr.Id). Fr.Id was separated by silica gel CC eluted with a CH_2Cl_2/MeOH gradient (100:0 to 100:20, v/v) to obtain five fractions (Fr.Id1 − Fr.Id5). Fr.Id1 was separated by sephadex LH-20 and followed by semi-preparative HPLC (75% MeCN in H_2O, 3.0 mL/min) to give **2** (8.8 mg, t_R = 13.5 min), **3** (7 mg, t_R = 21 min). Fr. Id2 was separated by sephadex LH-20 and followed by semi-preparative HPLC (60% MeCN in H_2O, 3.0 mL/min) to give **1** (6 mg, t_R = 16 min). Fr.Id3 was separated by silica gel CC (CH_2Cl_2/MeOH, 125:1), and followed by sephadex LH-20 (MeOH) to give **22** (70 mg). Fr.Id4 was separated by silica gel CC (CH_2Cl_2/MeOH, 50:1), sephadex LH-20 (MeOH), and followed by preparative TLC

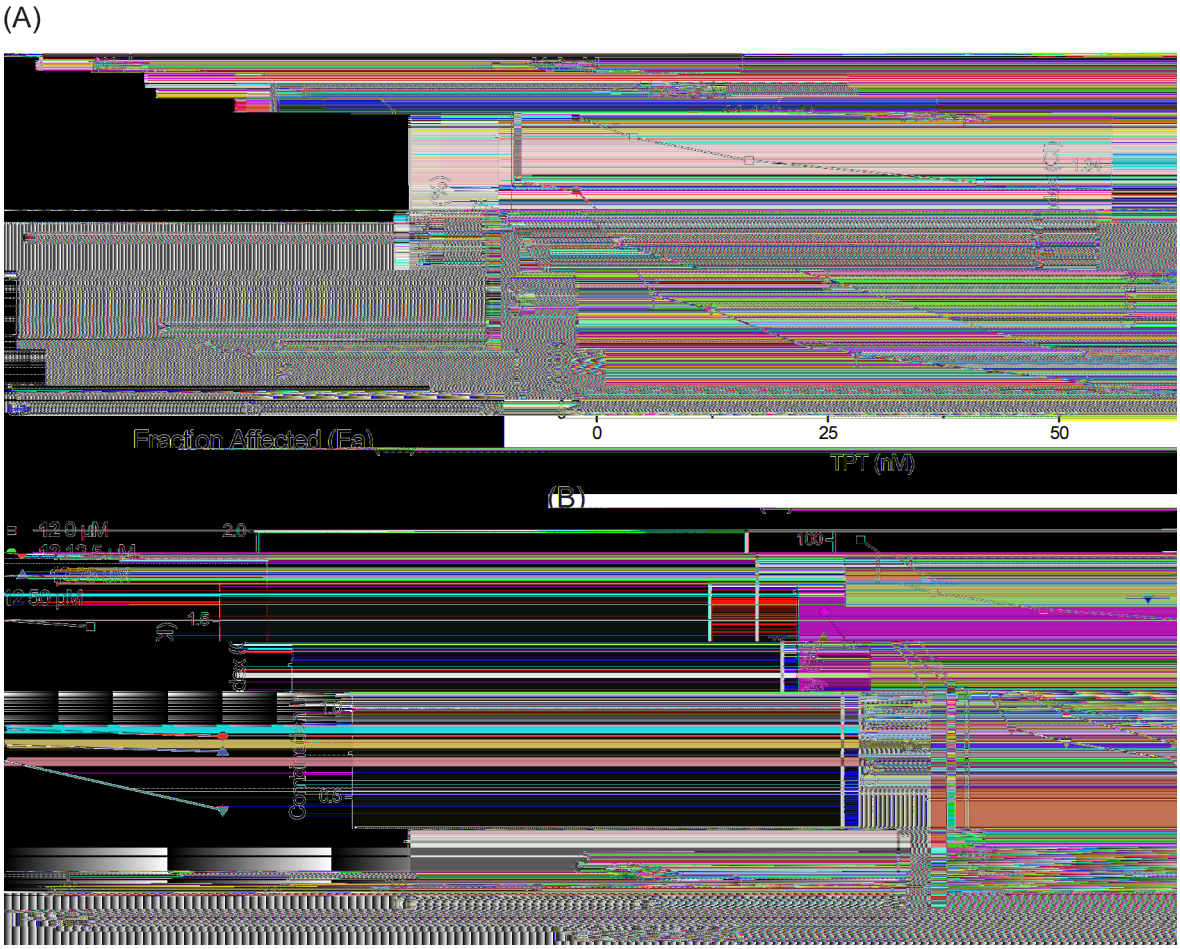

Fig. 5. Potentiation of the cytotoxic action of TPT in combination with **11** (A) and **12** (B) in MCF-7 cells. Left panels: dose response curves for combination treatment with TPT and **11** or **12**. Right panels: Combination Index (CI) vs. Fraction A□ected (Fa) plot for the dose response graphs in the left panels. CI < 1, synergism; CI < 0.3, strong synergism.

(CH_2Cl_2/MeOH, 70:1) to give **20** (20 mg), **24** (7.8 mg), and **26** (8 mg). Fr.Id5 was separated by sephadex LH-20 and further purified by silica gel CC (CH_2Cl_2/MeOH, 130:1, v/v) to give **13** (10 mg) and **15** (11.8 mg). Fr.Ic was subjected to silica gel CC (CH_2Cl_2/MeOH, 100:1 to 5:1, v/v) to give six fractions (Fr.Ic1 − Fr.Ic6). Fr.Ic2 was separated by sephadex LH-20 (MeOH), and followed by silica gel CC (CH_2Cl_2/MeOH, 1:0 to 100:1, v/v) to give **16** (20 mg), **17** (50 mg), and **27** (200 mg). Fr.Ic3 was separated by silica gel CC (CH_2Cl_2/MeOH, 100:1, v/v) to give **23** (14 mg), **25** (30 mg), **18** (10 mg), **19** (7 mg), **21** (8.6 mg), and **14** (18 mg). Fr.Ic4 was separated by semi-preparative HPLC (70% MeCN in H_2O, 3.0 mL/min) to give **11** (6 mg, t_R = 12 min). Fr.Ic5 was separated by semi-preparative HPLC (75% MeCN in H_2O, 3.0 mL/min) to give **12** (3 mg, t_R = 15 min). Fr.H was separated by MCI gel CC (MeOH/H_2O, 50:50 to 100:0, v/v) to obtain three fractions (Fr.H1 − Fr.H3). Fr.H2 was separated by silica gel CC (CH_2Cl_2) to give two subfractions (Fr.H2a − H2bFr.). Fr.H2a was separated by silica gel CC (petroleum ether/CH_2Cl_2, 1:1, v/v), and followed by sephadex LH-20 (MeOH) to give **4** (12 mg) and **5** (9 mg). Fr.H2b was separated by sephadex LH-20 (MeOH), and followed by silica gel CC (petroleum ether/CH_2Cl_2, 3:1, v/v) to give **6** (18 mg), **9** (7 mg), and **10** (3.8 mg). Fr.H3 was separated by sephadex LH-20 (MeOH) and RP-18 silica gel CC (83% MeOH in H_2O, v/v) to give **8** (9 mg) and **7** (4.8 mg).

4.3.1. Isodopene a (*1*)

White powder; mp 159.7–161.3 °C; [α] − 32.3 (*c* 0.3, MeCN); UV (MeCN) λ_{max} (log ε) 217 (3.20) nm; ECD (MeCN) 212 ($\Delta\varepsilon$ – 6.94) nm; IR (KBr) ν_{max}: 3374, 2919, 2852, 1762, 1707, and 1668 cm^{-1}. ^1H NMR (500 MHz, $CDCl_3$) and ^{13}C NMR (125 MHz, $CDCl_3$) date see Table 1. HRESIMS *m/z* 337.1771 [M + Na]$^+$ (calcd for $C_{20}H_{26}O_3Na^+$, 337.1774).

4.3.2. Isodopene B (*13*)

White powder; mp 182.9–184.6 °C; [α] + 65 (*c* 0.3, MeCN); UV (MeCN) λ_{max} (log ε) 227 (3.10) nm; ECD (MeCN) 187 ($\Delta\varepsilon$ + 18.31), 223 ($\Delta\varepsilon$ – 2.24) nm; IR (KBr) ν_{max}: 3337, 2954, 2921, 2852, and 1736 cm^{-1}. ^1H NMR (500 MHz, $CDCl_3$) and ^{13}C NMR (125 MHz, $CDCl_3$) date see Table 2. HRESIMS *m/z* 525.3560 [M + Na]$^+$ (calcd for $C_{31}H_{50}O_5Na^+$, 525.3550).

4.4. TOP1-mediated relaxation assay

All isolates were tested for the TOP1 inhibitory activity using TOP1-mediated relaxation assay.[31] Briefly, the reaction mixture (20 μL) containing 1 μL of supercoiled pBR322 DNA (0.5 μg/μL) in Relaxation Bu□er (10 mM Tris-HCl, pH 7.5, 50 mM KCl, 5 mM $MgCl_2$, 15 μg/mL BSA, 40 μg/mL DTT) was incubated with 1 unit of calf thymus TOP1 in the absence or presence of the tested compounds for 30 min at 37 °C. Then the reaction solution was added 6 × loading bu□er (4 μL), and was analyzed using a 0.8% agarose gel in TBE bu□er at 4.6 V/cm for 1.5 h. The gel was stained with 1 × gel red for 30 min and subsequently visualized with a UV transilluminator.

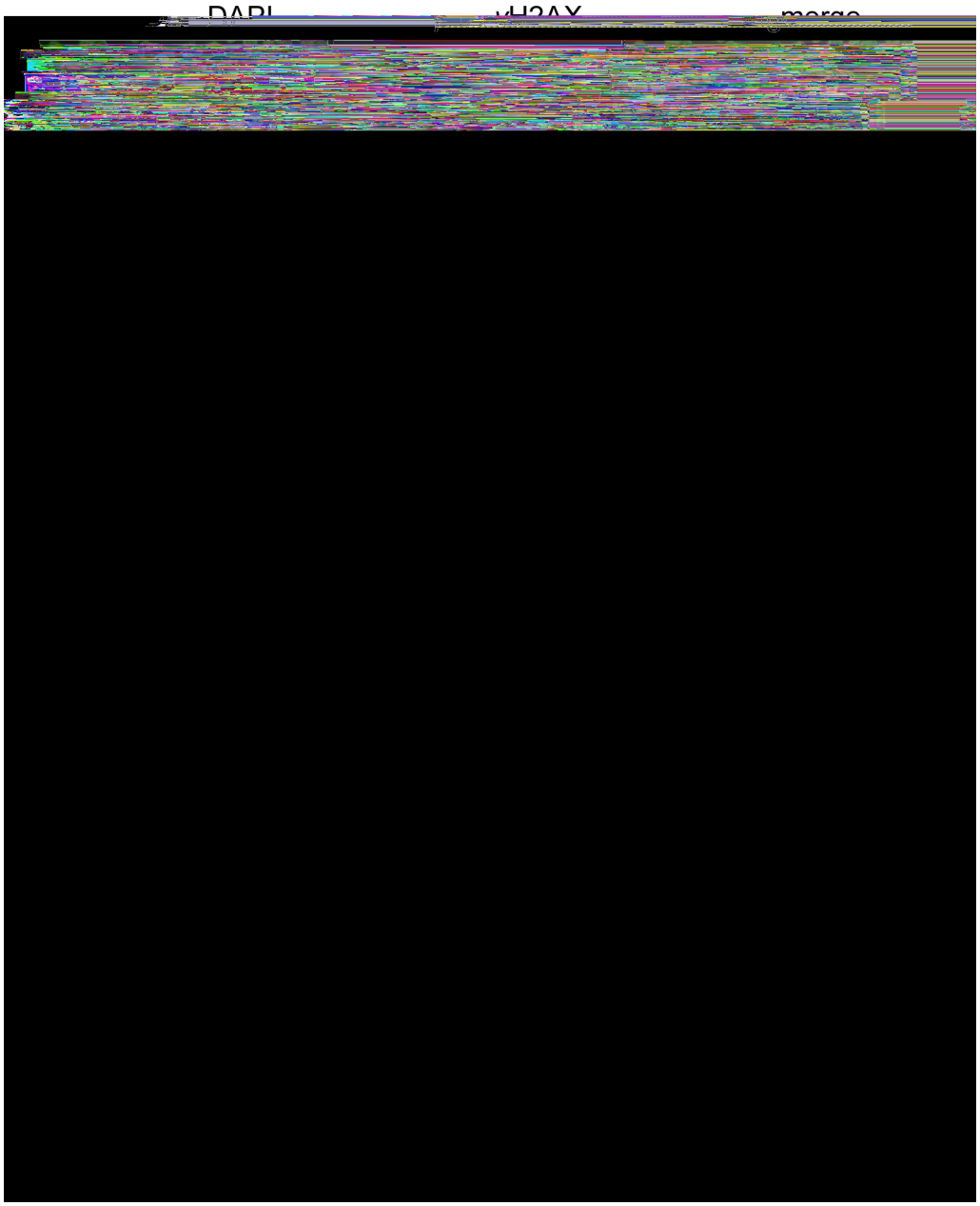

Fig. 6. Fluorescence microscopy detection of *γ*H2AX foci formation in MCF-7 cells. Cells were treated with CPT (0.5 μM) or the compounds **8** and **16** (9 μM) for 12 h.

4.5. TOP1-mediated cleavage assay

TOP1-mediated cleavage assay was carried out as mentioned before.[32] The reaction mixture (20 μL) containing 1 μL of supercoiled pBR322 DNA (0.5 μg/μL) and 10 units of calf thymus TOP1 in Relaxation Bu□er was incubated for 30 min at 37 °C. Then, the reaction solution was added with 4 μL of proteinase K (5.5 mg/mL) and incubated at 55 °C for 15 min. The reaction was terminated by the addition of 5 μL 6 × loading bu□er and was analyzed using a 0.8% agarose gel in TBE bu□er at 3 V/cm for 30 min. The gel was stained with ethidium bromide (EB, 0.125 μg/mL) in TBE bu□er for 30 min. Finally, the gel was run in TBE bu□er for another 30 min and was visualized with a UV transilluminator.

4.6. TOP1-mediated EMSA

TOP1-mediated DNA mobility shift analysis (EMSA) assay was used to evaluate whether the compounds hampered the binding of TOP1 to DNA.[33] Supercoiled pBR322 DNA (1 μL, 0.1 μg/μL) in 20 μL of Relaxation Bu□er was incubated with 4 units of TOP1 in the absence or presence of the tested compounds at 37 °C for 0.5 h. Then, the reaction solution was added with 4 μL 6 × loading bu□er and was analyzed using a 0.8% agarose gel with 1% EB in TBE bu□er at 0.8 V/cm for 6.5 h. The gel was visualized with a UV transilluminator.

4.7. TDP1 inhibition assay

The TDP1 fluorescence assay was conducted according to the reported method.[34] Briefly, the reaction mixture (50 μL) containing 20 μL of TDP1 solution [0.02 μL of purified TDP1 (100 nM) in 10 mM Tris-HCl, pH 7.5, 50 mM KCl, 1 mM EDTA, 1 mM DTT] was dispensed into a white 384-well plate. The tested compound solution in DMSO (5 μL) was pinned into assay plates. The solution was incubated at 37 °C for 30 min. Then, the plate was read by molecular devices at Ex_{485}/Em_{510} nm to identify false-positive compounds that had autofluorescence. The linear oligonucleotide substrate (5′-*FAM*-AGGATCTAAAAGACTT-BHQ-

3′, 25 μL, 35 nM) was dispensed into the wells to start the reaction. The plate was immediately read three times at Ex_{485}/Em_{510} nm. TDP1 inhibition percentage was calculated by comparing the rate of enhancement in fluorescence intensity for the compound-treated wells to that of DMSO control wells.

4.8. Cell culture and cytotoxicity assays

The cells were cultured on DMEM or RPMI-1640 medium at 37 °C in a humidified atmosphere with 5% CO_2. The cytotoxicity of compounds **1**–**27** was evaluated through MTT assay against three human cancer cell lines (breast cancer MCF-7, non-small cell lung cancer A549, and colon cancer HCT116). The cancer cells were treated with the compounds (predissolved in DMSO) at a five-dose assay ranging from 0.01 to 100 μM concentration for 72 h. MTT solution (20 μL, 2.5 mg/mL) in PBS bu□er was added. After being incubated for 4 h, the formazan crystal formed in the well was dissolved in 100 μL of DMSO for optical density at 570 nm. The GI_{50} value was calculated by nonlinear regression analysis (GraphPad Prism). Every experiment was conducted for three independent times.

4.9. Synergistic e ect

The drug combination experiments were measured by through MTT assay.[35] MCF-7 cells were treated with the tested compounds and TOP1 inhibitor topotecan for 72 h at 37 °C, and then measured by MTT assay. The combination index (CI) values were calculated by chou-talalay method (calcusyn software).

4.10. γH2AX detection

γH2AX staining was performed according to the reported method.[36] MCF-7 cells (5×10^4 cells/mL) were grown in culture medium and treated with the tested compounds for 12 h. After incubation, cells were fixed in 4% paraformaldehyde/PBS for 15 min at 25 °C, then permeabilized with 0.5% triton-X100/PBS at 37 °C for 30 min, and finally blocked with 5% goat serum/PBS at 37 °C for 3 h. Immunofluorescence assay was performed using standard methods, and the slides were incubated alternately with phospho-γH2AX (Cell Signaling Technology) at 37 °C overnight. The cover slips were washed six times with blocking bu□er and then incubated with anti-rabbit alexa 488-conjugated antibody (A21206, Life Technology) and 2 μg/mL of 4′,6-diamidino-2-phenylindole (DAPI, Invitrogen) at 37 °C for 2 h. The dishes were again washed six times with blocking bu□er. Digital images were recorded using a FLUOVIEW FV3000 (Olympus, Japan) and analyzed with FV31S-SW software.

Declaration of Competing Interest

The authors declare that they have no known competing financial interests or personal relationships that could have appeared to influence the work reported in this paper.

Acknowledgements

This work is supported by the National Natural Science Foundation of China, China (No. 81703668), Guangdong Basic and Applied Basic Research Foundation, China (Nos. 2019A1515011317 and 2017A030310396), Guangdong Provincial Key Laboratory of Construction Foundation, China (No. 2017B030314030), and Foundation of State Key Laboratory of Phytochemistry and Plant Resources in West China, China (No. P2017-KF06).

Appendix A. Supplementary material

IR, CD, HRESIMS, and NMR (^{1}H NMR, ^{13}C NMR, DEPT135, ^{1}H-^{1}H COSY, HSQC, HMBC and NOESY) spectra of Isodopene A (**1**) and B (**13**).

Supplementary data to this article can be found online at https://doi.org/10.1016/j.bmc.2020.115527.

References

1. Stewart L, Redinbo MR, Qiu X, et al. A Model for the Mechanism of Human Topoisomerase I. *Science.* 1998;279:1534–1541.
2. Pommier Y. Topoisomerase I inhibitors: Camptothecins and beyond. *Nat Rev Cancer.* 2006;6:789–802.
3. Pommier Y. DNA topoisomerase I Inhibitors: Chemistry, biology, and interfacial inhibition. *Chem Rev.* 2009;109:2894–2902.
4. Pommier Y, Leo E, Zhang H, et al. DNA topoisomerases and their poisoning by anticancer and antibacterial drugs. *Chem Biol.* 2010;17:421–433.
5. Pommier Y, Sun Y, Huang SYN, et al. Roles of eukaryotic topoisomerases in transcription, replication and genomic stability. *Nat Rev Mol Cell Biol.* 2016;17:703–721.
6. Choi SH, Tsuchida Y, Yang HW. Oral versus intraperitoneal administration of irinotecan in the treatment of human neuroblastoma in nude mice. *Cancer Lett.* 1998;124:15–21.
7. Brogden RN, Wiseman LR, Noble S. Topotecan: A review of its potential in advanced ovarian cancer. *Drugs.* 1998;56:709–723.
8. Bracher F, Tremmel T. From Lead to Drug Utilizing a Mannich Reaction: The Topotecan Story. *Arch Pharm.* 2017;350:1–8.
9. Wu N, Wu XW, Agama K, et al. A novel DNA topoisomerase i inhibitor with di□erent mechanism from camptothecin induces G2/M phase cell cycle arrest to K562 cells. *Biochemistry.* 2010;49:10131–10136.
10. Ganguly A, Das B, Roy A, et al. Betulinic acid, a catalytic inhibitor of topoisomerase I, inhibits reactive oxygen species-mediated apoptotic topoisomerase I-DNA cleavable complex formation in prostate cancer cells but does not a□ect the process of cell death. *Cancer Res.* 2007;67:11848–11858.
11. Qin XJ, Yu Q, Yan H, et al. Meroterpenoids with Antitumor Activities from *Guava* (Psidium guajava). *J Agric Food Chem.* 2017;65:4993–4999.
12. Qin XJ, Jin LY, Yu Q, et al. Eucalypglobulusals A-J, Formyl-Phloroglucinol-Terpene Meroterpenoids from *Eucalyptus globulus* Fruits. *J Nat Prod.* 2018;81:2638–2646.
13. Interthal H, Pouliot JJ, Champoux JJ. The tyrosyl-DNA phosphodiesterase Tdp1 is a member of the phospholipase D superfamily. *Proc Natl Acad Sci U S A.* 2001;98:12009–12014.
14. Dexheimer TS, Antony S, Marchand C, et al. Tyrosyl-DNA Phosphodiesterase as a Target for Anticancer Therapy. *Anticancer Agents Med Chem.* 2008;8:381–389.
15. Barthelmes HU, Habermeyer M, Christensen MO, et al. TDP1 overexpression in human cells counteracts DNA damage mediated by topoisomerases I and II. *J Biol Chem.* 2004;279:55618–55625.
16. Zakharenko A, Luzina O, Koval O, et al. Tyrosyl-DNA Phosphodiesterase 1 Inhibitors: Usnic Acid Enamines Enhance the Cytotoxic E□ect of Camptothecin. *J Nat Prod.* 2016;79:2961–2967.
17. Zhang XR, Wang HW, Tang WL, et al. Discovery, Synthesis, and Evaluation of Oxynitidine Derivatives as Dual Inhibitors of DNA Topoisomerase IB (TOP1) and Tyrosyl-DNA Phosphodiesterase 1 (TDP1), and Potential Antitumor Agents. *J Med Chem.* 2018;61:9908–9930.
18. Laev SS, Salakhutdinov NF, Lavrik OI. Tyrosyl-DNA phosphodiesterase inhibitors: Progress and potential. *Bioorganic Med Chem.* 2016;24:5017–5027.
19. Huang SY, Pommier Y, Marchand C. Tyrosyl-DNA Phosdiesterase 1 (Tdp1) Inhibitors. *Expert Opin Ther Pat.* 2011;21:1285–1292.
20. Nguyen TX, Morrell A, Conda-Sheridan M, et al. Synthesis and biological evaluation of the first dual tyrosyl-DNA phosphodiesterase i (Tdp1)-topoisomerase i (Top1) inhibitors. *J Med Chem.* 2012;55:4457–4478.
21. Flora of China Editorial Committee. Flora of China. Sciences Press. 1977; 66: 436–438.
22. Wu R, Geiduschek EP. Distinctive protein requirements of replication dependent and uncoupled bacteriophage T4 late gene expression. *J Virol.* 1977;24:436–443.
23. Zhang Y, Wang K, Chen H, et al. Anti-inflammatory lignans and phenylethanoid glycosides from the root of *Isodon ternifolius* (D.Don) Kudô. *Phytochemistry.* 2018;153:36–47.
24. Li Y, Wang Y, Wang S, et al. Oridonin phosphate-induced autophagy e□ectively enhances cell apoptosis of human breast cancer cells. *Med Oncol.* 2015;32:1–8.
25. Bao R, Shu Y, Wu X, et al. Oridonin induces apoptosis and cell cycle arrest of gallbladder cancer cells via the mitochondrial pathway. *BMC Cancer.* 2014;14:1–13.
26. Zhou GB, Kang H, Wang L, et al. Oridonin, a diterpenoid extracted from medicinal herbs, targets AML1-ETO fusion protein and shows potent antitumor activity with low adverse e□ects on t(8;21) leukemia in vitro and in vivo. *Blood.* 2007;109:3441–3450.
27. Shi M, Lu XJ, Zhang J, et al. Oridonin, a novel lysine acetyltransferases inhibitor, inhibits proliferation and induces apoptosis in gastric cancer cells through p53-and caspase-3-mediated mechanisms. *Oncotarget.* 2016;7:22623–22631.
28. Tsai SJ, Yin MC. Antioxidative and anti-inflammatory protection of oleanolic acid and ursolic acid in PC12 cells. *J Food Sci.* 2008;73:174–178.
29. Ramos AA, Pereira-Wilson C, Collins AR. Protective e□ects of Ursolic acid and Luteolin against oxidative DNA damage include enhancement of DNA repair in Caco-2 cells. *Mutat Res Fundam Mol Mech Mutagen.* 2010;692:6–11.

30. Kassi E, Papoutsi Z, Pratsinis H, et al. Ursolic acid, a naturally occurring triterpenoid, demonstrates anticancer activity on human prostate cancer cells. *J Cancer Res Clin Oncol.* 2007;133:493–500.
31. Liu LF, Miller KG. Eukaryotic DNA topoisomerases: Two forms of type I DNA topoisomerases from HeLa cell nuclei. *Proc Natl Acad Sci U S A.* 1981;78:3487–3491.
32. Hsiang YH, Hertzberg R, Hecht S, et al. Camptothecin induces protein-linked DNA breaks via mammalian DNA topoisomerase I. *J Biol Chem.* 1985;260:14873–14878.
33. Pommier Y, Covey JM, Kerngan D, et al. DNA unwinding and inhibition of mouse leukemia L1210 DNA topoisomerase I by intercalators. *Nucleic Acids Res.* 1987;15:6713–6731.
34. Dean RA, Fam HK, An J, et al. Identification of a putative tdp1 inhibitor (CD00509) by in vitro and cell-based assays. *J Biomol Screen.* 2014;19:1372–1382.
35. Kiselev E, Ravji A, Kankanala J, et al. Novel deazaflavin tyrosyl-DNA phosphodiesterase 2 (TDP2) inhibitors. *DNA Repair (Amst).* 2020;85:102747.
36. Sooryakumar D, Dexheimer TS, Teicher B, et al. Molecular and cellular pharmacology of the novel noncamptothecin topoisomerase I inhibitor, Genz-644282. *Mol Cancer Ther.* 2011;10:1490–1499.
37. Chen L, Yang Q, Hu K, Isoforrethins A-D, et al. four ent-abietane diterpenoids from *Isodon forrestii* var. forrestii. *Fitoterapia.* 2019;134:158–164.
38. Qin S, Chen SH, Guo YW, et al. Diterpenoids of *Isodon macrophylla*. *Helv Chim Acta.* 2007;90:2041–2046.
39. Cambie RC, Cox RE, Sidwell D. Phenolic diterpenoids of *podocarpus ferrugineus* and other podocarps. *Phytochemistry.* 1984;23:333–336.
40. Zhou XL, Xiao CJ, Bin Wu.L, et al. Five new terpenoids from the rhizomes of *Isodon adenantha*. *J Asian Nat Prod Res.* 2014;16:555–564.
41. Nagashima F, Toyota M, Asakawa Y. Terpenoids from some *Japanese liverworts*. *Phytochemistry.* 1990;29:2169–2174.
42. Devkota KP, Ratnayake R, Colburn NH, et al. Inhibitors of the oncogenic transcription factor AP-1 from *Podocarpus latifolius*. *J Nat Prod.* 2011;74:374–377.
43. Zhao J, Zhu HJ, Zhou XJ, et al. Diterpenoids from the feces of *Trogopterus xanthipes*. *J Nat Prod.* 2010;73:865–869.
44.